Biochimica et Biophysica Acta, 1142 (1993) 311–320

BBABIO 43817

Energy transfer dynamics of an isolated light harvesting complex of Photosystem I from spinach: time-resolved fluorescence measurements at 295 K and 77 K

Ishita Mukerji and Kenneth Sauer

Department of Chemistry and Structural Biology Division, Lawrence Berkeley Laboratory, University of California, Berkeley, CA (USA)

(Received 25 September 1992)

Key words: Chlorophyll; Energy transfer; Fluorescence; Light harvesting complex I; Photosystem I

Time-resolved fluorescence relaxation measurements have been performed at 295 K and 77 K on a preparation of the light-harvesting complex of Photosystem I (LHCI) containing about 100 chlorophylls (Chl) per complex. At both temperatures five exponential components were required to fit the data. The resulting determined lifetimes are 30 ps, 200 ps, 1.0 ns, 3.3 ns and 6.5 ns. Previous steady-state fluorescence measurements demonstrated that the emission at 735 nm increases dramatically upon cooling to 77 K. Time-resolved fluorescence measurements performed at 77 K reveal the presence of two risetimes for emission between 700 and 750 nm. These results are consistent with an efficient trap for electronic excitation existing at longer wavelengths than the absorption maximum of P700, the reaction center of Photosystem I (PS I). Excitation of Chl *b* results in a relative amplitude enhancement of decay components emitting between 720 and 750 nm. This confirms that Chl *b* is specifically associated with long wavelength emitters in Photosystem I.

Introduction

The function of a light-harvesting system in a photosynthetic apparatus is to collect light energy and effectively channel it to the reaction center (RC), where charge separation occurs. In photosynthetic organisms, light-harvesting systems consist of arrays of pigment which are either covalently or non-covalently attached to a protein matrix. Fluorescence spectroscopy has been used extensively to investigate the mechanism of excitation transport to the RC in these pigment-protein systems. With the advent of ultrafast laser systems and increasing knowledge of photosynthetic pigment-protein structures the paths of excitation migration within a light-harvesting array and the mechanism of excitation transfer can be studied in greater detail [1–4].

Photosystem I (PS I) is a particularly interesting system to study because the emission spectrum exhibits a pronounced temperature dependence. The emission maximum shifts from 690 nm to 735 nm upon cooling to 77 K, and this shift is accompanied by a 20-fold increase in the fluorescence yield [5]. This dramatic increase in fluorescence at longer wavelengths implicates the existence of low energy pigments within the antenna system. These pigments comprise less than 5% of the total antenna population as evidenced by absorption spectra. Steady-state fluorescence measurements on PS I demonstrate that approximately half of the fluorescence emission at 295 K occurs at lower energy than the absorption maximum of the reaction center. The existence of this far-red emission is suggestive of an uphill flow of energy to the RC. The presence of low energy pigments within PS I which give rise to fluorescence at 720 nm and 735 nm has been previously postulated, and their absorbance is thought to occur at 697 nm (C697) and 705 nm (C705) [6].

In an attempt to define the function of these special pigments with respect to energy transfer within an antenna array, we have undertaken a study of an isolated light-harvesting antenna complex of PS I (LHCI). Biochemical fractionation techniques coupled with spectroscopic studies have demonstrated that the origin of the long wavelength emission (F735) in PS I in higher plants is associated with this peripheral light

Correspondence to: K. Sauer, Department of Chemistry and Structural Biology Division, Lawrence Berkeley Laboratory, University of California, Berkeley, CA 94720, USA.

Abbreviations: Chl, chlorophyll; fwhm, full width half maximum; LHCI, light harvesting complex I; LHCII, light harvesting complex II; PS, Photosystem; RC, reaction center; SDS-PAGE, sodium dodecyl sulfate-polyacrylamide gel electrophoresis.

harvesting antenna complex [7–9]. Although its specific fluorescence characteristics differ from species to species, in all cases the fluorescence from the peripheral antenna system occurs at longer wavelength than the absorption maximum of the primary donor, P700. In PS I particles isolated from cyanobacteria or in cyanobacterial mutants lacking Photosystem II, fluorescence emission at room temperature is observed at 690 nm with a large shoulder at 720 nm [10]. In the thermophilic strain, *Synechococcus* sp., even at room temperature the peak emission is at 720 nm, with a shoulder at 690 nm [11,12]. Thus, the evolution of PS I in plants has resulted in the elaboration of its light harvesting system to include an antenna system which fluoresces at significantly lower energy (F735) than the absorption maximum of the reaction center.

Recent spectroscopic studies on a long wavelength pigment in the light harvesting array of *Rb. sphaeroides* and *R. rubrum* are indicative that these special pigments provide a mechanism for focussing energy prior to transfer to the RC [13,14]. From steady-state emission spectra of LHCI and the holocomplex, PS I-200, it is evident that a significant amount of the excitation is reaching these low energy pigments at room temperature [5,15]. Multiple rise times observed in time-resolved fluorescence data on LHCI presented in this study demonstrate that the pigments with low energy excited states are very effective at trapping excitation, especially at lower temperatures. Recent time-resolved fluorescence results of Werst et al. [16] on a mutant strain of *C. reinhardtii* demonstrate that, as the temperature is decreased, recovered lifetimes increase in magnitude for emission above 710 nm. Kinetic results on isolated LHCI indicate that an increase in amplitude of longer lived components at 77 K leads to the increase in fluorescence yield at 720 nm and 735 nm observed in both time-resolved and steady-state fluorescence measurements [5,15]. A comparison of results obtained on LHCI and PS I-200 is suggestive that LHCI completely dominates the energy transfer kinetics in the holocomplex at lower temperatures. This study reports the time-resolved fluorescence from an isolated preparation of LHCI from higher plants.

Materials and Methods

LHCI was isolated from spinach PS I-200 following the method of Haworth et al. [8] with some minor modifications. PS I-200 fractions were collected from linear sucrose density gradients as described [5]. These fractions were assayed by steady-state fluorescence to insure complete separation from LHCII and were then pooled and stored at −20°C for a period no longer than one month. PS I-200 material from two or three preparations was often collected prior to proceeding to the isolation of LHCI, to obtain enough material for spectroscopic measurements. The pooled fractions of PS I-200 were dialyzed against 0.05 M sorbitol at 4°C in the dark for 18 h. The aggregated material was pelleted by centrifugation ($12\,000 \times g$; 10 min). Pellets were then diluted with ice cold H_2O to a Chl concentration of 0.5 mg/ml. At this time dodecyl β-D-maltoside (Calbiochem) and Zwittergent-16 (Calbiochem) were added to the solution to give final concentrations of 1.5 mg/ml and 2.0 mg/ml, respectively. The detergent mixture was shaken for 1 h in the dark at 0°C and immediately loaded onto a 0.1–1.0 M linear sucrose density gradient containing 0.025% dodecyl β-D-maltoside and 0.02 M Tricine (pH 7.8). The gradients were centrifuged at $85\,000 \times g$ for 18.5 h. The isolated antenna pigment band was located near the top of the gradient immediately below a free Chl band. A second band on the gradient contained the reaction centers. The low concentrations of detergents used insured that the isolated LHCI remained relatively intact. Purity of the material was assessed by SDS-PAGE. The Bio-Rad silver stain procedure was used for detection of protein bands and demonstrated the complete absence of reaction center in these preparations. Purity of the material was also assessed by steady-state fluorescence and absorption.

Steady-state fluorescence measurements were performed using a SPEX Fluorolog 2 model 212 spectrofluorimeter with a wavelength resolution of ±2 nm. All emission scans were corrected for emission monochromator and photomultiplier tube wavelength dependence. Fluorescence decays were measured by time-correlated single photon counting. Picosecond pulses were provided by a tunable cavity-dumped dye laser (Spectra Physics 375 and Spectra Physics 341) synchronously pumped by an Ar ion laser (Spectra Physics 171). DCM (Exciton) was used as the lasing dye. Pulses were issued at a repetition rate of 823 kHz. Fluorescence was collected at right angles by an 85 mm camera lens (Nikon) and then sent through a sheet polarizer set at 54.7° to eliminate any anisotropic bias in the measurement. The emission wavelength was selected by a double monochromator (Instruments, SA) with a 4 nm bandwidth and detected by a Hamamatsu R2809U-11 microchannel plate photomultiplier tube. The instrument response function, measured by scattering the excitation beam with a solution of non-dairy creamer in H_2O, had an fwhm of 50–60 ps. The channel width for data collection was typically about 25 ps. Data analysis was performed as previously described [5]. The fitting range for the data analysis was approx. 27 ns. The decay component amplitudes at each wavelength were corrected for data collection time, excitation intensity and the wavelength dependence of the emission monochromator and detector. Decay component amplitudes were also normalized to the number of photons absorbed at the two different

excitation wavelengths. Relative amplitudes are defined such that:

$$\sum_i \alpha_i = 1$$

Results

The isolated light-harvesting complex of PS I from higher plants contains four polypeptides with masses ranging from 21 to 26 kDa, and the 21 kDa component is sometimes observed as a doublet [17]. Biochemical studies have shown that the majority of the Chl *b* is located on one polypeptide [18,19]. These polypeptides bind approx. 100 Chl molecules. Using the green alga *Chlamydomonas reinhardtii* Schuster et al. [20] determined a stoichiometric ratio of 3:8:5/core complex for the 27, 26 and 25 kDa subunits of LHCI. For the 22 kDa subunit which putatively binds all the Chl, a stoichiometry of 10 copies/core complex was determined. The core complex contains the 2 large proteins (80 kDa), which bind the RC and early electron transfer components, and 3 low molecular weight polypeptides. In contrast to the green algae studies, Bruce and Malkin [21] determined a ratio of 2 copies of the 23 kDa LHCI subunit/core complex in *Lemna gibba*, an aquatic higher plant. In both studies autoradiography was used to determine the stoichiometric ratios. From electron microscopy images [22] it was postulated that LHCI forms a shell of eight polypeptides around the core polypeptides of PS I, based upon mass/volume ratio comparisons of PS I-100 and PS I-200 isolated from spinach. The stoichiometric ratio of LHCI polypeptides to the core complex is relatively unclear; however, from the results of Boekema et al. [22] it can be estimated that each LHCI subunit binds approx. 12 Chl molecules.

Chl concentrations were determined using the method of Arnon [23], and the LHCI isolated in our laboratory was found to have a Chl *a*/Chl *b* ratio between 3:1 and 4:1. Absorption spectra confirm the presence of Chl *b* with pronounced shoulders at 650 and 472 nm (Fig. 1). Absorption between 700 and 730 nm in LHCI is relatively low, implying that the absorption of low energy pigments is small in comparison with that of the rest of the antenna Chl. At room temperature LHCI has an emission maximum at 685 nm (F685) with a broad shoulder ranging from 710–740 nm. At 77 K a dramatic increase in fluorescence at 733 nm (F735) relative to that at 685 nm is observed, as shown in Fig. 2.

Time-resolved fluorescence measurements at 295 K

Time-resolved fluorescence spectroscopy on the LHCI complex was performed to probe changes in

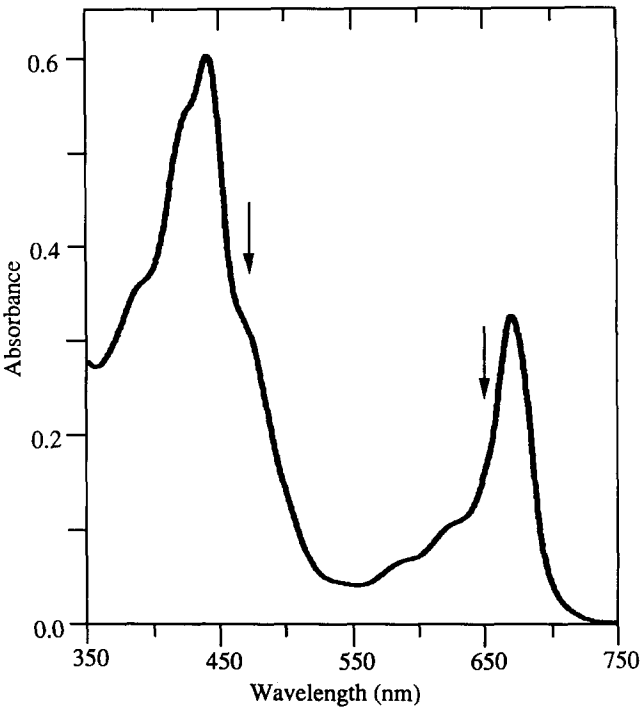

Fig. 1. Absorption spectrum of LHCI from spinach. Sample was diluted in 0.05 M Tricine (pH 7.8) to 0.01 mg Chl/ml. Absorption path was 0.4 cm. The absorption maxima occur at 440 nm and 672 nm. Chl *b* absorption at 472 nm and 650 nm indicated by arrows.

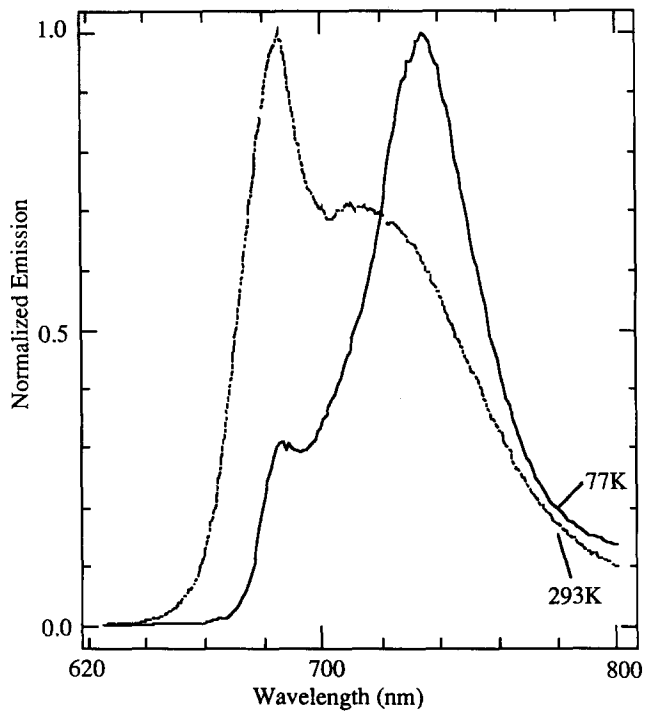

Fig. 2. Steady state fluorescence emission of LHCI at 293 K and 77 K. Excitation done at 435 nm. Sample originally in 0.1–0.2 M sucrose diluted 5-fold. 293 K: sample dilution done with 0.05 M Tricine (pH 7.8). 77 K: sample dilution done with 40% 0.05 M Tricine (pH 7.8), 60% glycerol. Spectra are normalized to maximum peak height.

excitation transfer as a function of temperature and excitation wavelength. Measurements were done at two different excitation wavelengths, 670 nm and 650 nm, absorption maxima of Chl *a* and Chl *b*, respectively. At 295 K and 77 K fluorescence decays were measured from 680 nm to 750 nm at 5 nm intervals. Single-wavelength decay analysis demonstrated that the lifetimes obtained were substantially independent of emission wavelength; therefore, the global analysis method was applied to the data [24,25]. By inspection of the weighted residuals and the χ^2 value, we determined that at both 295 K and 77 K at least five components were necessary to fit the fluorescence decays. Fig. 3 depicts representative residuals from global analysis fits using either a four- or a five-component model. Some features of the instrument response are not successfully deconvoluted leading to a slight distortion in the residuals. However, at both temperatures five-component fits consistently gave lower χ^2 values at all emission wavelengths, indicating that this model satisfied the data better than a four-component model.

Excitation of Chl a. The decay component amplitudes plotted as a function of emission wavelength for excitation at 670 nm are shown in Fig. 4. A relatively fast 30 ps component exhibits its amplitude maximum at 680 nm (see Table I). The amplitude of that component drops dramatically when the emission is measured at longer wavelengths (Fig. 4). A second component, with a lifetime of about 200 ps has a very broad amplitude maximum which peaks at 710–720 nm, contributing at most 50% of the total amplitude. We also detect several longer-lived components. This is not surprising in the absence of any photosynthetic reaction centers in these preparations. A 1.0 ns component is observed which contributes 10% to the overall amplitude. A 3.3 ns component is greatest at 680 nm, yet adds less than 5% to the amplitude. We also resolve a 6.5 ns component which appears to peak at 680 nm, but its relative amplitude is less than 1%. The amplitude of this decay component is correlated with the observation of peaks in the steady state fluorescence spectrum at 660 nm and 680 nm. Therefore, we attribute this longest lived component to a small amount of Chl released during the isolation process. The 3.3 ns component, despite its small amplitude, comprises approx. 40% of the integrated yield owing to its long lifetime.

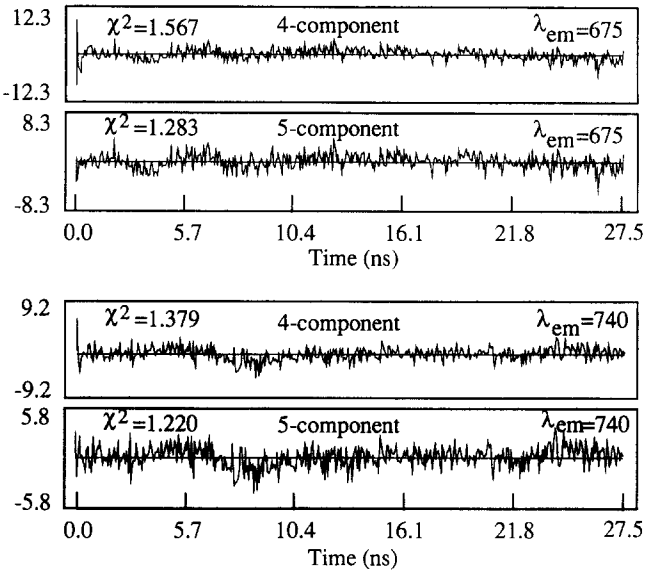

Fig. 3. Comparison of residuals from 4- and 5-component global analysis. Representative weighted residuals from global analysis of emission decays using either a 4- or a 5-exponential model. Residuals from analyses using a 4-exponential model are displayed above residuals from the 5-exponential model at the same emission wavelength.

TABLE I

Lifetimes and amplitude maxima obtained from global analysis of fluorescence kinetics of LHCI

Decay components	1	2	3	4	5
$T = 295$ K					
Lifetimes (ns)	0.03 ± 0.02	0.21 ± 0.06	1.0 ± 0.2	3.3 ± 0.6	6.5 ± 1.2
Amplitude maximum (nm)	680–685	710–720	685–690 720–725	680	680–690
$T = 77$ K					
Lifetimes (ns)	0.04 ± 0.01	0.20 ± 0.06	1.1 ± 0.1	3.6 ± 0.25	6.7 ± 0.5
Positive amplitude maximum (nm)	680	685	715–720	730	680–685 735
Negative amplitude maximum (nm)	725–735	735	–	–	–

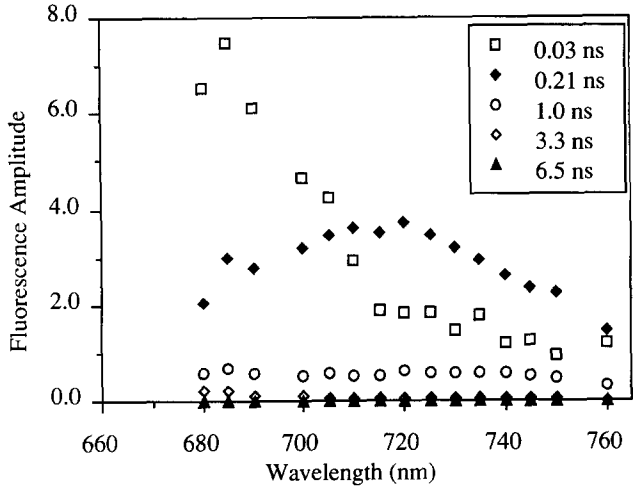

Fig. 4. Decay-associated spectrum of LHCI. Excitation wavelength at 670 nm. Data taken at 295 K. Decays were fit to a sum of five exponentials using the global analysis method. Amplitudes are plotted as a function of emission wavelength. Samples were diluted with 0.05 M Tricine (pH 7.8) to give [Chl] = 0.01 mg/ml.

Excitation of Chl b. Fig. 5 depicts the decay component amplitudes plotted as a function of wavelength for $\lambda_{ex} = 650$ nm at 295 K. Within error the lifetimes are identical to those observed for $\lambda_{ex} = 670$ nm. We detect two major changes in the amplitudes as a function of emission wavelength. For emission at 680 nm the relative amplitudes of the 30 ps and 200 ps components have decreased approx. 25% compared with excitation at 670 nm. At 735 nm the relative amplitude of the 200 ps component has decreased to 50% of that obtained with 670 nm excitation, while the relative amplitude of the 30 ps component remains at 75% of the 670 nm excitation value. Conversely, the increase in emission between 710–740 nm, as observed in the steady-state emission spectrum [15], arises from a 3-fold increase in

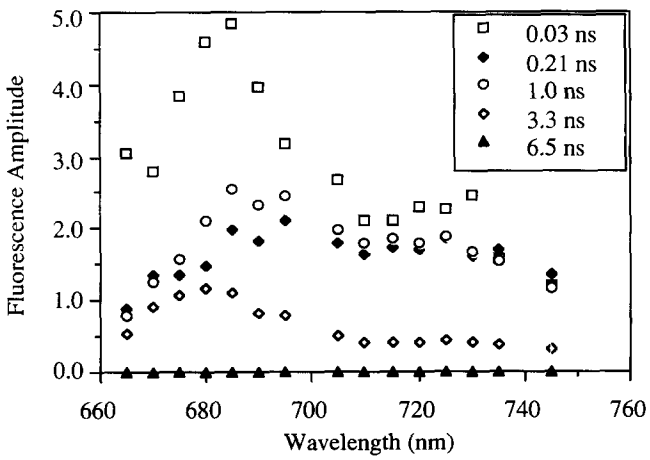

Fig. 5. Decay associated spectrum of LHC-1. Excitation done at 650 nm. Decays were fit to a sum of five exponentials using the global analysis method. Data were taken at 295 K. Amplitudes are plotted as a function of emission wavelength. Sample preparation as in Fig. 4.

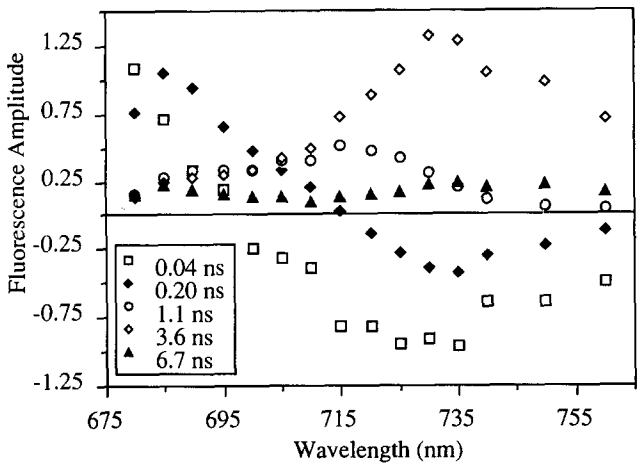

Fig. 6. Decay-associated spectrum of LHCI. Excitation was done at 665 nm. Data were taken at 77 K. Data analysis as in Figs. 4 and 5. Samples were diluted to < 0.1 absorbance at 675 nm and were frozen to a cracked glass in 60% glycerol, 40% 0.05 M Tricine (pH 7.8).

relative amplitude of the 1.0 ns and 3.3 ns decay components. The 1.0 ns component displays broad maxima at 685 nm and 725 nm and its contribution to the total amplitude is relatively higher at 725 nm than at 685 nm. Although the 3.3 ns component contributes significantly to emission between 710 and 740 nm, its amplitude maximum occurs at 680 nm (see Table I). In LHCI the relative quantum yield for fluorescence does not vary significantly over the entire absorption range. Steady-state emission measurements of the quantum yield with either 650 nm or 670 nm excitation gave approximately the same value within the error of the measurement [12]. We suggest that the enhanced relative amplitudes of the 1.0 ns and the 3.3 ns decay components upon excitation at the Chl *b* absorption maximum probably reflects the coupling between Chl *b* and long wavelength emitters and not an overall increase in the efficiency for fluorescence.

Time-resolved fluorescence spectroscopy at 77 K

Excitation of Chl a. In Fig. 6 the decay-associated spectrum for $\lambda_{ex} = 665$ nm taken at 77 K is plotted as a function of wavelength. The choice of 665 nm as the excitation wavelength served to suppress contributions from scattering to the emission detected at 680 nm. A similar set of lifetimes of the individual decay components at the lower temperature is extracted by global analysis; the decay component amplitudes, however, display a dramatic difference in wavelength dependence compared with those at room temperature. At the shorter emission wavelengths (680–685 nm) the results are similar to those observed at room temperature, in the sense that the amplitudes of the 40 ps and 200 ps decay components are dominant. This is the region of the emission spectrum where the fluorescence increase relative to that at room temperature is

smaller [15]. At longer wavelengths, however, the results of the global analysis are very different from those at room temperature. These amplitude changes are presumably associated with the significant increase in F735 observed in the steady state fluorescence spectra when the temperature is lowered to 77 K (Fig. 2). The 40 ps component peaks at 680 nm and contributes approx. 40% of the amplitude, similar to what was observed at 295 K. This component crosses over to a negative amplitude (rise component) at 695–700 nm and then exhibits a broad negative amplitude maximum between 725–735 nm (see Table I). A negative amplitude or rise, as opposed to decay, is indicative of fluorescence induction resulting from excitation transfer within these complex antenna systems. The 200 ps component exhibits a maximum at 685 nm and accounts for approx. 40% of the total amplitude. It also displays rise behavior, crossing over to a negative amplitude between 715–720 nm and exhibiting a negative maximum at 735 nm. The amplitude of the 1.0 ns component at 77 K exhibits a maximum at 720 nm and then drops significantly at longer wavelengths.

The presence of two rise components in the decay kinetics argues for the presence of an efficient trap for excitation energy from 710 to 740 nm. We observe that the 3.6 ns component completely dominates both the yield and the amplitude at longer wavelengths, reaching a maximum at 730 nm. At 77 K the wavelength dependence of the amplitude of the 3.6 ns component demonstrates that it acts as a sink for energy transfer within the antenna system. The 6.5 ns component displays an amplitude maximum at 685 nm and also at 735 nm. The wavelength dependence of the 6.5 ns component at 77 K possibly reflects the presence of two long-lived decay components which are not fully resolved by the global analysis method.

Excitation of Chl b. The maxima of the decay component amplitudes at 77 K for $\lambda_{ex} = 650$ nm are similar to those observed for $\lambda_{ex} = 665$ nm, although the intensities are different (Fig. 7). The primary difference observed is the enhanced emission ratio F730/F685, which results from several factors. At 730 nm the amplitudes of the 3.6 ns and the 1.0 ns decay components have increased by a factor of 2 relative to those obtained with 665 nm excitation. Kinetic data then support previously obtained results on LHCI which demonstrate that Chl *b* sensitizes emission at longer wavelengths [15]. The fluorescence yield can be calculated using the following equation:

$$k_F\left[\frac{\sum_i \alpha_i \tau_i}{\sum_i \alpha_i}\right] = \Phi_F$$

where α_i is the amplitude and τ_i is the lifetime of the ith decay component. For both RT and 77 K data a summation of the yield of each decay component, results in a calculated spectrum (Fig. 8) that is essentially identical to the steady state emission spectrum (Fig. 2).

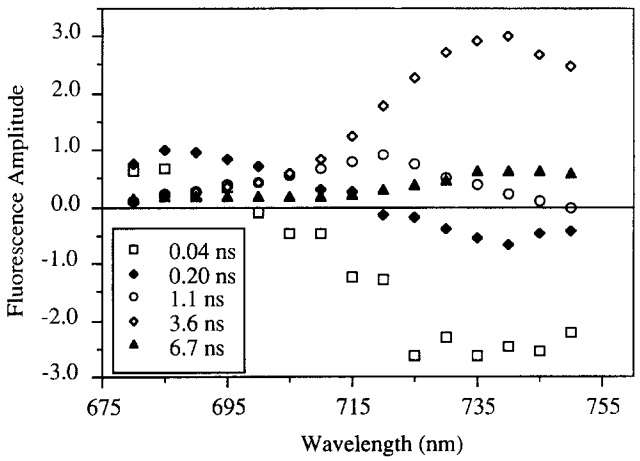

Fig. 7. Decay-associated spectrum of LHCI. Excitation was done at 650 nm. Data were taken at 77 K. Data analysis as described in Figs. 4 and 5. Sample preparation as in Fig. 6.

For the data presented in Figs. 6 and 7 it was observed that for 735 nm emission the rise amplitude of the 40 ps component with Chl *b* excitation has increased by a factor of 2.75 when compared with the rise amplitude obtained with excitation at 665 nm. Assuming that the absorption due to Chl *b* at 665 nm is negligible then this large increase in rise amplitude with 650 nm excitation is suggestive of the presence of an additional fast component which is not resolved in the current experiment. This component would have kinetics either equivalent to or faster than the 40 ps decay component and would emit at shorter wavelengths than 680 nm. These characteristics would be

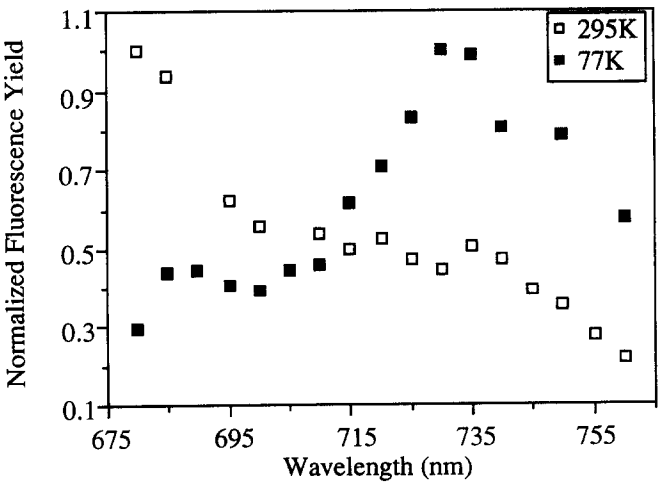

Fig. 8. Calculated total fluorescence yield of LHCI (described in text). Data were taken at 295 K and 77 K. Excitation was done at 670 nm (295 K) or 665 nm (77 K). Yields normalized to peak maxima. For comparison with steady state data see Fig. 2.

consistent with an emitting pool primarily composed of Chl *b* chromophores which emit at 665 nm and rapidly transfer excitation to F720 and F735, as suggested by low temperature excitation spectra [15]. Alternatively, rather than the appearance of a larger rise amplitude, it is possible that we are observing a suppression of the 40 ps decay amplitude which would allow the rise amplitude to predominate, also leading to the observed experimental result that the net rise amplitude has increased for 650 nm excitation.

We note that the shorter lifetimes reported (Table I) have a large error associated with them. Some of the uncertainty in recovered lifetimes can be attributed to the amount of free Chl, which was not constant from preparation to preparation. At 77 K, where the contribution of free Chl to the overall yield is less, the error in lifetime is also correspondingly less (see Table I).

For the time-resolved emission spectra the main observations are: (1) five decay components are required to satisfy the data at room temperature and 77 K. (2) The wavelength dependence at 77 K is significantly different from what is observed at 295 K, which is consistent with the pronounced temperature dependence detected in the steady-state emission spectra. (3) At 77 K excitation is efficiently transferred to the 3.6 ns component, as evidenced by the two risetimes observed in the far-red region of the emission spectrum and by the dominance of the 3.6 ns component in the long wavelength fluorescence yield. (4) Chl *b* excitation enhances the amplitudes of the 1.0 and 3.3 ns (3.6 ns at 77 K) decay components relative to those observed upon excitation of Chl *a*.

Discussion

The kinetic data that we have obtained on LHCI may be compared with previously reported results on the PS I-200 complex at 77 K [5]. The wavelength-dependent amplitude behavior in the antenna complex, however, differs from that of the holocomplex. More prominent fluorescence induction is observed in the antenna complex, and it is likely that at 77 K in the absence of the reaction center the fraction of excitation reaching far red emitting pigments is enhanced in LHCI relative to what is observed in PS I-200. The fluorescence quantum yield of LHCI is 10-fold greater than that measured for PS I-200 at room temperature [12]. This demonstrates that in the holocomplex excitation energy absorbed by LHCI is efficiently quenched by the reaction center. LHCI represents a significant functional element of the light harvesting array of PS I.

The mean tau of LHCI can be expressed as:

$$\tau_{\text{mean}} = \frac{\sum_i \alpha_i \tau_i^2}{\sum_i \alpha_i \tau_i}$$

This amplitude-weighted mean lifetime increases for emission at longer wavelengths. Thus, in LHCI at 295 K the mean tau changes from 1.27 ns at 680 nm to 2.45 ns at 730 nm. Additionally, the mean lifetime increases with decreasing temperature; at 77 K τ_{mean} is 3.70 ns at 680 nm and 4.50 ns at 730 nm. These differences in lifetime are not sufficient to account for the increase in yield observed in the steady state fluorescence spectrum [15]. Coupled with the increases in τ_{mean}, an increase in amplitude of longer-lived components which exhibit maxima between 720 and 740 nm is also observed. Increases at 77 K in decay amplitudes of the longer-lived components relative to room temperature spectra can be attributed to a reduced amount of back energy transfer from F735 to C672 at the lower temperature.

Werst et al. [16] have performed time-resolved fluorescence measurements on both whole cells and isolated PS I-particles from a mutant strain of *Chlamydomonas reinhardtii* which lacks PS II. They report that the lifetimes of the components emitting between 680 nm and 710 nm remain relatively independent of temperature; whereas at 720 nm the recovered lifetimes increase as a function of decreasing temperature. The increase in total fluorescence yield at 720 nm at lower temperature results mainly from an increase in yield of the intermediate and long-lived components, caused by their increase in lifetime. Although from our measurements it is not possible to specifically address the dependence of lifetime on temperature, our results qualitatively agree with those of Werst et al. [16] In both studies the increase in total fluorescence yield from 720 nm to 735 nm results from an increase in yield of the intermediate and long-lived decay components. Werst et al. [16] do not observe any rise components in their measurements; however, the free Chl present in their preparations could be obscuring the detection of these components.

The 40 ps and 200 ps components of the fluorescence decay observed from 680 to 695 nm appear as inductions in the long wavelength region at 77 K. The wavelength dependence of these components is suggestive of energy being transferred from the major Chl *a*/*b* components of LHCI to C705 or other far red absorbing pigments. The two rise components exhibit cross-over points at 695 nm and 715 nm, indicative of a downhill flow of energy to the sink. At 295 K a risetime is not detected at longer wavelengths. Between 710 and 740 nm the observed 30 ps component presumably reflects the superposition of a rapid decay of fluorescence in the tail of F685 and an equally rapid rise in F735. The observed amplitude corresponds to the algebraic sum of these two components. Thus, in the high-temperature limit only a net decay is seen, whereas in the low-temperature limit only a rise is detected.

Experiments by Holzwarth et al. in which a very fast

risetime was observed were conducted at 5°C [11,26]. At that temperature the amplitude of the rise component is larger and possibly more easily detected. The decay amplitude of the 30 ps (40 ps at 77 K) component peaks between 680 and 685 nm. If a normal Stokes' shift is assumed, then this emission can be correlated with the absorption maximum of LHCI at 672 nm. Therefore, it is reasonable that the 30 ps decay component is associated with the majority of the Chl in the antenna complex. This decay component is similar to fast decay components observed in PS I particles isolated from spinach and cyanobacteria [11,16,26]. Faster lifetimes have also been observed in polarized photobleaching experiments done on similar PS I preparations [27]. The very fast decay probably reflects the rapid redistribution of energy to other spectral forms within the antenna complex. A theoretical model describing the temperature dependence of PS I energy transfer and trapping in terms of pigment spectral types has been developed and reported [28]. The intensity of the steady state emission at 735 nm also supports the postulate that energy absorbed at 672 nm is rapidly transferred to longer wavelength pigments. In the LHCI complex the emission shoulder from 710–740 nm is approximately two-thirds the height of the main peak. Thus, even at room temperature a substantial amount of the excitation is reaching the low energy emitters. Steady-state fluorescence measurements of LHCI over a relatively narrow temperature range have demonstrated that these low energy pigments dissipate an increasing proportion of the excitation as the temperature is lowered [15].

In a pump-probe spectroscopy study done on PS I-200 particles Lyle and Struve [29] report that photobleaching decay lifetimes do not increase dramatically with lower temperature. By monitoring isotropic and anisotropic photobleaching decays of antenna Chl from RT to 38 K at 680 nm, they observe that the anisotropic decays are much more temperature dependent than the isotropic decays. Secondly, they detect little change in lifetime from 292 K to 77 K, but observe a dramatic order of magnitude increase in lifetime from 77 K to 38 K. The authors attribute the relatively weak temperature dependence of the isotropic decays to equilibration of various antenna Chl *a* spectral forms, which occurs on a faster time scale (< 1 ps) than that of their experiment. Our results support a rapid equilibration of Chl *a* spectral forms, although not a rapid equilibration between Chl *a* and Chl *b*. Lyle and Struve [29] did not perform measurements at 650 nm; therefore, the effect of Chl *b* was not assessed.

From the decay-associated spectra of LHCI at 77 K (Figs. 6 and 7) it can be seen that the 1.1 ns component peaks at 720 nm. From this behavior we postulate the presence of an intermediate pigment pool between F685 and F735, similar to the one(s) present in the PS I core antenna. It was previously thought that this antenna component was associated only with the RC-containing polypeptides. Kinetic data on LHCI are suggestive that F720 (C697) is also a component of the peripheral antenna. However, we cannot rule out the possibility that the wavelength dependence of the 1.1 ns component at 77 K results from the sum of rise and decay components which do not have maxima at 720 nm. The emission at 735 nm is dominated by the 3.6 ns component, associating this decay with the longest wavelength emitter of LHCI at 77 K.

Excitation at 650 nm enhances the amplitude of longer-lived decay components relative to excitation at 670 nm (665 nm at 77 K). From these results and previously reported fluorescence excitation spectra [5,15] it is evident that Chl *b* is closely connected to chromophores which emit in the 710–740 nm region. Additionally, time-resolved fluorescence data taken at 77 K with excitation at 650 nm provide indirect evidence for the existence of a predominantly Chl *b* antenna pool. From the wavelength dependence of the amplitude of the 40 ps component it can be inferred that Chl *b* rapidly transfers excitation to the low energy pigments, C697 and C705.

At room temperature an 80–100 ps component is observed in PS I-200 which is not present in the kinetics of LHCI. This absence confirms our previous assignment of this component to lower energy emitting pigments (F720) predominantly associated with reaction center-containing polypeptides [5]. In *Chlamydomonas reinhardtii* mutants Lin and Knox [30] found a lifetime with a similar wavelength dependence, which they attribute to excitation transfer between LHCII and LHCI. Since our experiments are done on isolated preparations it is not possible to assess excitation transfer from LHCII; however, from our results it appears that this component is closely associated with the reaction center, P700.

The observed fluorescence kinetics of LHCI is considerably more complex than expected. A possible explanation for the observed complexity lies in the nature of the isolated LHCI. Recent results of Allen and Staehelin [31] using a native green gel system resolve multiple PS I-LHCI complexes. The relative concentrations of these complexes do not increase with larger relative amounts of detergent, indicating that the smaller complexes are not derivatives of a larger complex but rather represent heterogeneous species present in the thylakoid membrane.

From a three-dimensional structure of LHCII as determined by electron diffraction and electron microscopy [4] the proximity of chromophores in a monomer is suggestive that delocalized excitonic coupling may occur on a faster time-scale than could be resolved by our instrumentation if a similar situation is present in LHCI. Consistent with the proposed struc-

ture of LHCII, Eads et al. [32] have measured a Chl *b* to Chl *a* energy transfer rate of 0.5 ± 0.2 ps in LHCII. If LHCI proves to have structural features similar to LHCII, then the energy transfer processes that we resolve probably occur between pools of pigment that have been previously equilibrated. These results would then be consistent with a pebble mosaic model, in which cluster equilibration occurs on a faster time scale than equilibration between clusters.

Proposed model for excitation transfer in LHCI

Based on these time-resolved fluorescence relaxation measurements we propose a model for excitation transfer within LHCI (Fig. 9). At 77 K forward transfer reactions dominate; whereas, at room temperature we suggest that a significant amount of back transfer is occurring. The model incorporates a distinct pool of chromophores containing mainly Chl *b*, which is strongly coupled to long wavelength emitters. This Chl *b* pool (C650) also transfers energy to a predominantly Chl *a* pool (C672). We suggest that at least 50% of the initial excitation absorbed at C650 is rapidly transferred to C697 and C705. The pools described represent clusters of chromophores which have been previously equilibrated by excitonic interactions. The majority of absorbed excitation occurs at C672, which emits between 685 and 695 nm. C672 excitation is also transferred to low energy pigments. As stated earlier it is possible that the 720 nm amplitude maximum observed for the 200 ps decay component (295 K) and the 1.1 ns decay component (77 K) arises fortuitously from a sum of rise and decay components with other amplitude maxima. Therefore, because our measurements do not definitively demonstrate the presence of C697 (F720), we propose two models for excitation transfer in LHCI, one in which C697 is present (Fig. 9b) and one where it is not (Fig. 9a). Both models incorporate specific transfer steps from C650 to C705, which leads to the enhanced emission at 735 nm observed experimentally upon excitation of Chl *b*.

Excitation transfer from LHCI to the reaction center

From measurements of the relative fluorescence quantum yield and a comparison of the tau mean of PS I-200 (0.06–0.135 ns) and LHCI (1.27–2.45 ns) it is clear that, when it is associated with the RC complex, LHCI effectively transfers energy to the reaction center antenna at room temperature. In PS I-200 if LHCI does not completely relax prior to excitation transfer to the RC then it is possible that C672 excitation is directly transferred to antenna chromophores located close to the RC.

However, if LHCI does relax prior to excitation transfer to the reaction center antenna then C705 would be implicated as a conduit for excitation transfer from LHCI to the RC. Thus, the function of C705 (F735) remains an unanswered question. From these results it is clear that C705 is very effective at trapping electronic excitation in LHCI. Similar pigments have been detected in both purple bacteria [13,14] and LHCII [33] arguing that these pigments are endemic to the structure of a light harvesting antenna. It has been suggested that B896 in purple bacteria [13,14] acts to focus excitation energy prior to transfer to the RC. Simulations done by Werst et al. [16] and Jia et al. [28] show the best agreement with experimental results for PS I particles isolated from *C. reinhardtii*, when a model with a random arrangement of chromophores including one or two low-energy pigments placed close to the RC is used. The relatively long lifetimes observed in this study can be associated with these low energy pigments; we postulate that such long-lived species would be useful for storing excitation prior to transfer to the RC. The implication of this model is that C705 and the RC must be in close proximity, thereby constraining the geometry of LHCI around the RC core polypeptides. Both Peter et al. [34] and Bassi and Simpson [35] have isolated PS I complexes which consist of LHCI Chl *b*-containing polypeptides and RC-containing polypeptides. Fluorescence from the Bassi and Simpson complex (LHCI-730) occurred at

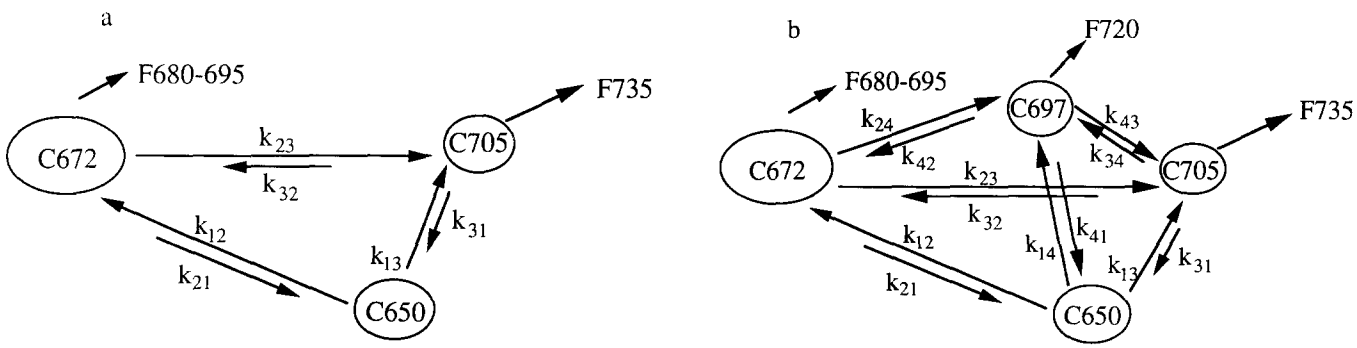

Fig. 9. Proposed model of transfer energetics within LHCI. (a) Model consists of three emitting species, emission maxima as shown. (b) Model consists of four emitting species, specifically including C697 (F720). In both models at 295 K significant back transfer reactions are occurring, and at 77 K forward transfer reactions predominate.

730 nm, intimating the presence of C705. Thus, it can be inferred that the polypeptides which contain C705 are coupled very tightly to RC-containing polypeptides. Certainly, the room temperature fluorescence in PS I-200 appears to be quenched relative to that of LHCI as shown by the order of magnitude difference in relative quantum yield and the differences in τ_{mean}. Further experimentation on LHCI-730 or a similar complex should address the role of C705 in the excitation transfer dynamics in PS I.

Acknowledgements

We would like to thank Dr. Alfred Holzwarth of the Max Planck Institute of Radiation Chemistry, Mülheim/Ruhr for generously supplying the data analysis programs. We are also grateful to Dr. Holger Dau for many helpful and stimulating discussions. This work was supported by the Director, Office of Energy Research, Office of Basic Energy Sciences, Energy Biosciences Division of the U.S. Department of Energy under Contract No. DE-AC03-76SF00098.

References

1 Holzwarth, A.R. (1991) in The Chlorophylls (Scheer, H., ed.), pp. 1125–1151, CRC Press, Boca Raton.
2 Struve, W.S. (1990) J. Opt. Soc. Am. B 7, 1586–1594.
3 Schirmer, T., Bode, W. and Huber, R. (1987) J. Mol. Biol 196, 677–695.
4 Kühlbrandt, W. and Wang, D.N. (1991) Nature 350, 130–134.
5 Mukerji, I. and Sauer K. (1989) in Photosynthesis (Briggs, W.R., ed.) pp. 105–122, Alan R. Liss, New York.
6 Butler, W.L., Tredwell, C.J., Malkin, R. and Barber, J. (1979) Biochim. Biophys. Acta 545, 309–315.
7 Mullet, J.E., Burke, J.J. and Arntzen, C.J. (1980) Plant Physiol. 65, 814–822.
8 Haworth, P., Watson, J.L. and Arntzen, C.J. (1983) Biochim. Biophys. Acta 724, 151–158.
9 Lam, E., Ortiz, W. and Malkin R. (1986) FEBS Lett. 168, 10–14.
10 Wittmershaus, B.P., Woolf, V.M. and Vermaas, W.F.J. (1992) Photosynth. Res. 31, 75–87.
11 Holzwarth, A.R., Haehnel, W., Ratajczak, R., Bittersmann, E. and Schatz, G.H. (1990) in Current Research in Photosynthesis (Baltscheffsky, M., ed.), Vol. II, pp. 611–614, Kluwer, Dordrecht.
12 Mukerji, I. (1990) in Fluorescence Spectroscopy of Excitation Transfer in Photosystem I, PhD Thesis, Lawrence Berkeley Laboratory Report (LBL-30136), pp. 26–49, University of California, Berkeley.
13 Bergström, H., Van Grondelle, R. and Sundström, V. (1989) FEBS Lett. 250, 503–508.
14 Sundström, V. and Van Grondelle, R. (1990) J. Opt. Soc. Am. B. 7, 1595–1603.
15 Mukerji, I. and Sauer, K. (1990) in Current Research in Photosynthesis (Baltscheffsky, M., ed.), Vol. II, pp. 321–324, Kluwer, Dordrecht.
16 Werst, M., Jia, Y., Mets, L. and Fleming, G.R. (1992) Biophys. J. 61, 868–878.
17 Anandan, S., Vainstein, A. and Thornber, J.P. (1989) FEBS Lett. 256, 150–154.
18 Nechushtai, R., Peterson, C.C., Peter, G.F. and Thornber, J.P. (1987) Eur. J. Biochem. 164, 345–350.
19 Vainstein, A., Peterson, C.C. and Thornber, J.P. (1989) J. Biol. Chem. 264, 4058–4063.
20 Schuster, G., Nechushtai, R., Ferreira, P.C.G., Thornber, J.P. and Ohad, I. (1988) Eur. J. Biochem 177, 411–416.
21 Bruce, B.D. and Malkin, R. (1988) J. Biol. Chem. 263, 7302–7308.
22 Boekema, E.J., Wynn, R.M. and Malkin, R. (1990) Biochim. Biophys. Acta 1017, 49–56.
23 Arnon, D.I. (1949) Plant Physiol. 24, 1–15.
24 Wendler, J., John, W., Scheer, H. and Holzwarth, A.R. (1986) Photochem. Photobiol. 44, 79–85.
25 Knutson, J.R., Beechem, J.M. and Brand, L. (1983) Chem. Phys. Lett. 102, 501–507.
26 Holzwarth, A.R. (1990) in Current Research in Photosynthesis (Baltscheffsky, M., ed.), Vol. II, pp. 223–230, Kluwer, Dordrecht.
27 Causgrove, T.P., Yang, S. and Struve, W.S. (1989) J. Phys. Chem. 93, 6844–6850.
28 Jia, Y., Jean, J.M., Werst, M.M., Chan, C.-K. and Fleming, G.R. (1992) Biophys. J. 63, 259–273.
29 Lyle, P.A. and Struve, W.S. (1991) J. Phys. Chem. 95, 4152–4158.
30 Lin, S. and Knox, R.S. (1991) Photosynth. Res. 27, 157–168.
31 Allen, K.D. and Staehelin, L.A. (1991) Anal. Biochem. 194, 214–222.
32 Eads, D.D., Castner, E.W., Jr., Alberte, R.S., Mets, L. and Fleming, G.R. (1989) J. Phys. Chem. 93, 8271–8275.
33 Zucchelli, G., Jennings, R.C. and Garlaschi, F.M. (1990) J. Photochem. Photobiol. B: Biol. 6, 381–394.
34 Peter, G.F., Machold, O. and Thornber, J.P. (1988) in Plant Membranes: Structure, Assembly and Function (Harwood, J.L. and Walton, T.J., eds.), pp. 17–31, Biochemical Society, London.
35 Bassi, R. and Simpson, D. (1987) Eur. J. Biochem. 163, 221–230.